THE JOURNAL OF BIOLOGICAL CHEMISTRY VOL. 286, NO. 47, pp. 41069–41082, November 25, 2011

Novel Role for Pendrin in Orchestrating Bicarbonate Secretion in Cystic Fibrosis Transmembrane Conductance Regulator (CFTR)-expressing Airway Serous Cells*[S]

Received for publication, June 14, 2011, and in revised form, September 6, 2011 Published, JBC Papers in Press, September 13, 2011, DOI 10.1074/jbc.M111.266734

James P. Garnett[‡1], Emma Hickman[§], Rachel Burrows[§], Péter Hegyi[¶], László Tiszlavicz[‖], Alan W. Cuthbert[**], Peying Fong[‡‡], and Michael A. Gray[‡2]

From the [‡]Institute for Cell and Molecular Biosciences, Newcastle University, Newcastle upon Tyne NE2 4HH, United Kingdom, the [§]Novartis Institutes for Biomedical Research, Novartis Horsham Research Centre, Horsham, West Sussex, RH12 5AB, United Kingdom, the Departments of [¶]Medicine and [‖]Pathology, University of Szeged, Szeged H6701, Hungary, the [**]Department of Medicine, University of Cambridge, Addenbrooke's Hospital, Cambridge CB2 2QQ, United Kingdom, and the [‡‡]Department of Anatomy and Physiology, Kansas State University College of Veterinary Medicine, Manhattan, Kansas 66505

In most HCO_3^--secreting epithelial tissues, SLC26 Cl^-/HCO_3^- transporters work in concert with the cystic fibrosis transmembrane conductance regulator (CFTR) to regulate the magnitude and composition of the secreted fluid, a process that is vital for normal tissue function. By contrast, CFTR is regarded as the only exit pathway for HCO_3^- in the airways. Here we show that Cl^-/HCO_3^- anion exchange makes a major contribution to transcellular HCO_3^- transport in airway serous cells. Real-time measurement of intracellular pH from polarized cultures of human Calu-3 cells demonstrated cAMP/PKA-activated Cl^--dependent HCO_3^- transport across the luminal membrane via CFTR-dependent coupled Cl^-/HCO_3^- anion exchange. The pharmacological and functional profile of the luminal anion exchanger was consistent with SLC26A4 (pendrin), which was shown to be expressed by quantitative RT-PCR, Western blot, and immunofluorescence. Pendrin-mediated anion exchange activity was confirmed by shRNA pendrin knockdown (KD), which markedly reduced cAMP-activated Cl^-/HCO_3^- exchange. To establish the relative roles of CFTR and pendrin in net HCO_3^- secretion, transepithelial liquid secretion rate and liquid pH were measured in wild type, pendrin KD, and CFTR KD cells. cAMP/PKA increased the rate and pH of the secreted fluid. Inhibiting CFTR reduced the rate of liquid secretion but not the pH, whereas decreasing pendrin activity lowered pH with little effect on volume. These results establish that CFTR predominately controls the rate of liquid secretion, whereas pendrin regulates the composition of the secreted fluid and identifies a critical role for this anion exchanger in transcellular HCO_3^- secretion in airway serous cells.

HCO_3^- is a vital component of epithelial secretions. Despite the growing awareness of its importance in epithelial function, the molecular mechanism of HCO_3^- secretion remains incompletely understood. Via its buffering role, HCO_3^- controls the pH of the luminal microenvironment, a function particularly important to the physiology of many epithelial tissues, including the airways. Consistent with a role for HCO_3^- secretion in airway function, a previous study found the airway surface liquid to be acidic in cystic fibrosis (CF)[3] compared with normal cell cultures (1), and a similar finding was made in secretions from nasal submucosal glands (SMGs) from CF patients (2). Aberrant pH/HCO_3^- secretion probably contributes to CF lung pathogenesis in a number of fundamental ways. HCO_3^- is a chaotropic anion that facilitates efficient solubilization and transport of macromolecules, such as mucus (3). Also, the recent finding that HCO_3^- secretion is required for mucus secretion (4–6) and that mucin expansion and viscosity are regulated by HCO_3^- (7, 8) strongly suggests that adequate HCO_3^- is required for proper mucus homeostasis. In addition, acidic pH has been shown to reduce ciliary beat frequency (9) and impede bacterial killing by phagocytic cells (10, 11). Collectively, these consequences of inadequate HCO_3^- transport predispose the lungs to mucus blockage, bacterial infection, and disease, all hallmarks of the CF lung.

Current studies suggest that HCO_3^- exit (secretion) across the luminal plasma membrane of airway epithelial cells is mediated solely by the cystic fibrosis transmembrane conductance regulator (CFTR), the ion channel that is mutated in CF. Exactly how CFTR dysfunction leads to aberrant HCO_3^- secretion is unclear. In primary cultures of surface bronchial and tracheal epithelial cells from CF humans and pigs, a lack of CFTR is associated with reduced electrogenic HCO_3^- secretion (12, 13). Likewise, in *ex vivo* studies of liquid/mucus secretion from intact SMGs from a range of species, cAMP-stimulated fluid

* This work was supported by a Biotechnology and Biological Sciences Research Council-Industrial Collaborative Ph.D. Studentship Award BBS/S/M/2006/13134 (to J. P. G.).

[S] The on-line version of this article (available at http://www.jbc.org) contains supplemental Tables S1–S3 and Figs. S1–S6.

[1] Present address: Division of Biomedical Sciences, St George's, University of London, London SW17 0RE, United Kingdom.

[2] To whom correspondence should be addressed: Epithelial Research Group, Institute for Cell and Molecular Biosciences, Newcastle University, Newcastle upon Tyne NE2 4HH, United Kingdom. Tel.: 44-191-222-7592; Fax: 44-191-222-7424; E-mail: m.a.gray@ncl.ac.uk.

[3] The abbreviations used are: CF, cystic fibrosis; AE, anion exchange; CFTR, cystic fibrosis transmembrane conductance regulator; EBIO, 1-ethyl-2-benzimidazolinone; fsk, forskolin; H_2-DIDS, 4,4′-diisothiocyano-1,2-diphenylethane-2,2′-disulfonate; J_v, rate of liquid secretion; KD, knockdown; KRB, HCO_3^--buffered Krebs solution; NBC, Na^+-HCO_3^- cotransporter; ΔpH_{RA}, rate of reacidification; V_m, membrane potential; V_{te}, transepithelial resistance; SMG, submucosal gland; FRT, Fischer rat thyroid; $0Cl^-$, absence of Cl^-.

secretion depends on both Cl^- and HCO_3^- and was absent in CF glands (14–16). Furthermore, detailed studies of anion and fluid secretion from polarized cultures of human airway Calu-3 cells, a model of human tracheobronchial SMG serous cells, also concluded that CFTR was the sole mediator of apical Cl^- and HCO_3^- secretion (17–19). However, in many HCO_3^--secreting epithelia, including the pancreas (20), salivary glands (21), and gastrointestinal (22) and reproductive tracts (23), HCO_3^- secretion is mediated by CFTR and one or more Cl^-/HCO_3^- exchangers belonging to the SLC26 gene family. This family comprises 10 members, and their functional characterization indicates distinct patterns of anion specificity and transport modes. Furthermore, structural analyses indicate that CFTR and SLC26 transporters can physically interact through their regulatory and STAS domains, respectively (24), a process that is enhanced by PKA phosphorylation of the regulatory domain (24). In most cases, these molecular interactions synergize the transport activity of CFTR and the SLC26 exchanger, resulting in enhanced HCO_3^- and fluid secretion from epithelial tissues.

Therefore, SLC26 anion exchangers have a well documented role in HCO_3^- secretion in non-airway tissues. Human tracheal airway epithelial cells express abundant SLC26A3, whereas delF508 cells do not (25). Furthermore, RNA analysis has shown that human lungs also express SLC26A9 (26) which appears to act as a constitutively active CFTR-regulated Cl^- channel in cultured human bronchial epithelial cells (27). However, to date, it is unknown whether SLC26 proteins are involved in HCO_3^- secretion in the airways. Hence, the purpose of this study was to investigate the potential role of SLC26 Cl^-/HCO_3^- exchangers in transcellular HCO_3^- secretion in airway epithelial cells. Our results show for the first time that human airway serous cells possess a luminal cAMP/PKA-activated Cl^-/HCO_3^- exchanger that exhibits functional properties consistent with those of SLC26A4 (pendrin). Short hairpin RNA (shRNA)-mediated knockdown of pendrin expression significantly reduced Cl^-/HCO_3^- exchange activity and markedly lowered the HCO_3^- content of the secreted fluid. These studies therefore identify for the first time a critical role for pendrin in transcellular HCO_3^- secretion by airway serous cells.

EXPERIMENTAL PROCEDURES

Calu-3 Cell Culture—The human adenocarcinoma-derived cell line, Calu-3 (passages 20–50 (28)), was grown in Eagle's minimal essential medium plus 10% FCS, 2 mM L-glutamine, 100 units/ml penicillin, 100 μg/ml streptomycin, and 1% non-essential amino acids (Sigma) and incubated in humidified air containing 5% CO_2 at 37 °C. CFTR knockdown (KD) Calu-3 cells (29), SLC26A4, and cyclophilin B KD Calu-3 cells were cultured in the same media supplemented with Geneticin (CFTR KD, 400 μg/ml; G418; Sigma) or puromycin (10 μg/ml; Sigma), respectively. For experiments using polarized cells, Calu-3 cells were seeded onto clear Costar Transwell® or Snapwell® inserts (0.45-μm pore size, 1.12-cm^2 surface area) at 250,000 cells/cm^2, respectively. Calu-3 cells generally formed a confluent monolayer with a stable transepithelial resistance (V_{te}) of 700–900 ohms/cm^2 after 5 days of growth on Transwell inserts. Experiments were carried out 7–14 days postseeding.

Fischer Rat Thyroid (FRT) Cell Culture—Non-transfected FRT cells and FRT cells stably transfected with pendrin or CFTR were kindly provided by Drs. L. Galietta and O. Zegarra-Moran (University of Genoa, Italy) and generated as described previously (30). The cells were cultured in Coon's modified Ham's F-12 medium supplemented with 10% FCS, 2 mM L-glutamine, 100 units/ml penicillin, 100 μg/ml streptomycin, and 1% non-essential amino acids. For CFTR-transfected FRT cells, medium was supplemented with 0.75 mg/ml Geneticin (G418; Sigma) and 0.6 mg/ml zeocin (Sigma). Pendrin-transfected FRT cells were grown in medium supplemented with 1 mg/ml Geneticin and 0.5 mg/ml hygromycin (Sigma).

shRNA Knockdown of SLC26A4 in Calu-3 Cells—Individual SLC26A4 and cyclophilin B (control)-deficient Calu-3 cell lines were produced using lentivirus-mediated delivery of shRNA (Sigma MISSION) knockdown with a set of four different shRNA sequences (supplemental Table S1). Lentiviral transduction particles were applied at a multiplicity of infection ratio of 1. Transduced cells were selected 48 h post-transduction using 10 μg/ml puromycin. KD cell lines used for this study had V_{te} and growth patterns similar to that of WT Calu-3 cells.

Measurement of Intracellular pH—Cells were loaded with the pH-sensitive fluorescent dye 2′,7′-bis-(2-carboxyethyl)-5(6)-carboxyfluorescein acetoxymethyl ester (10 μM) for 45–60 min at 37 °C in a HEPES-buffered salt solution, which consisted of 130 mM NaCl, 5 mM KCl, 1 mM $MgCl_2$, 1 mM $CaCl_2$, 10 mM Na-HEPES, and 10 mM D-glucose set to pH 7.4. Transwells were placed in a perfusion chamber, mounted onto an inverted microscope stage (Nikon), and perfused with a HCO_3^--buffered Krebs solution (KRB), which consisted of 115 mM NaCl, 5 mM KCl, 25 mM $NaHCO_3$, 1 mM $MgCl_2$, 1 mM $CaCl_2$, and 10 mM D-glucose and adjusted to pH 7.4 by bubbling with a 95% O_2, 5% CO_2 mixture at 37 °C. Apical and basolateral bath volumes were 0.5 and 1 ml and were perfused at a rate of 3 and 6 ml/min, respectively. Intracellular pH (pH_i) was measured from 15–20 cells as described previously (31), using a Life Sciences Microfluorimeter System (Life Sciences Resources). Ratio values were calibrated to pH_i using the high K^+-nigericin method (10 μM), using K^+ solutions of various pH values from 5.6 to 8.6 (31). Mean changes in pH_i were estimated by calculating the average pH_i over 60 s (120 data points). The initial rate of pH_i change ($\Delta pH_i/\Delta t$) was calculated by linear regression fitted to a minimum of 40 data points. Total buffering capacity was estimated by the ammonium pulse technique, using the Henderson-Hasselbalch equation as described previously (31). The $\Delta pH_i/\Delta t$ values were converted to transmembrane efflux of HCO_3^- ($-J(B)$) using the equation, $-J(B)$ = rate of pH_i change × total buffering capacity. For high K^+ KRB, KCl was increased to 115 mM, and NaCl was reduced to 5 mM. For Cl^--free KRB, NaCl was substituted with sodium gluconate, with 6 mM calcium gluconate replacing 1 mM $CaCl_2$ to compensate for the Ca^{2+} buffering capacity of gluconate, and 5 mM KCl was replaced with 2.5 mM K_2SO_4. For Na^+-free KRB, 115 mM NMDG-Cl replaced NaCl, and 25 mM choline-HCO_3 replaced $NaHCO_3$. Atropine (10 μM) was included to block muscarinic receptors. Cl^--free HEPES-buffered solution consisted of 130 mM sodium gluconate, 2.5 mM K_2SO_4, 1 mM magnesium gluconate, 6 mM calcium gluconate, 10 mM HEPES (free acid), and 10 mM D-glucose. All

general chemicals were purchased from Sigma-Aldrich except for forskolin (Tocris), and GlyH-101 (Calbiochem).

Transepithelial Liquid Secretion Rates and pH Measurements—After washing confluent monolayers with PBS, to remove mucus, the rate of liquid secretion (J_v) was determined by applying 0.2 and 1 ml of Krebs solution to the apical and basolateral surfaces of the cells, respectively, with the desired agonist or inhibitors. Cells were placed in a humidified CO_2 incubator at 37 °C, and the volume of the apical fluid was measured using a calibrated micropipette after 24 h. For HCO_3^--free experiments, Transwells were bathed in HEPES-buffered solution and maintained in a humidified incubator at 37 °C without CO_2 gassing. Correction for evaporative apical volume loss (0.08 ± 0.02 μl/cm^2/h; $n = 12$) was determined empirically by measuring the reduction in apical volume from Transwells coated with silicone gel to stop fluid leakage across the membrane. The pH of 5% CO_2-saturated apical fluid was measured using a micro-pH electrode (Hamilton) within 60 s of removing individual Transwells from the incubator. Control experiments showed that pH drifted by 0.04 pH units/min using this approach.

Quantitative RT-PCR Analysis of SLC26 Gene Expression—Total RNA was isolated using the Qiagen RNeasy miniprep kit and quantified using the Bioanalyzer 2100 and RNA total nanochips and reagents (Agilent Technologies). cDNA synthesis was performed with 20 ng/ml total RNA/sample using the GeneAmp RT-PCR kit (Applied Biosystems). A mixed tissue standard was generated from total RNA (liver, spleen, kidney, lung, testis, pancreas, brain, and fetal brain; purchased individually from Clontech). Quantitative RT-PCR (Taqman) analysis was used to measure *SLC26* gene expression, using previously optimized primers and probes (Applied Biosystems, Assays-on-Demand; supplemental Table S2). Amplicons were designed to span intron-exon boundaries to preclude possible amplification of genomic DNA sequences. Reactions were performed in 96-well optical plates and analyzed on the ABI PRISM 7700 (Applied Biosystems) using the following program: 50 °C for 2 min and 95 °C for 10 min followed by 45 cycles of 95 °C for 15 s and 60 °C for 1 min. Data were quantified relative to the standard curve for each gene. Expression was normalized to *GAPDH* and expressed as percentage relative to the standard curve.

Immunocytochemistry—Calu-3 cells grown on Transwells were fixed and permeabilized with cold 100% methanol (−20 °C) for 15 min on ice. Samples were blocked with 3% horse serum for 1 h at room temperature and then incubated with a mouse polyclonal anti-pendrin (Abnova) at 1:200 overnight at 4 °C. After blocking with 3% goat serum for 1 h at room temperature, samples were incubated with a goat Alexa Fluor 488-coupled anti-mouse secondary antibody (Invitrogen) at 1:1000 in 3% goat serum. The samples were also stained for zona occludens 1 (ZO-1), using a rabbit anti-ZO-1 antibody (1:500; Invitrogen) and a goat anti-rabbit secondary antibody (1:1000; Red Alexa Fluor 568, Invitrogen). Negative controls omitted primary antibody. Images were collected by confocal laser-scanning microscopy, using a Leica TCS-NT system (Leica UK Ltd.) equipped with a ×100 oil immersion lens, using appropriate excitation and emission filter sets for dual fluorophore detection. Leica software was used to capture images, under identical conditions of imaging, illumination intensity, and photomultiplier settings.

Statistical Analysis—Results are presented as mean ± S.E., where n indicates the number of experiments. Statistical analysis was performed with GraphPad Prism software (GraphPad Software Inc.), using either a paired Student's t test or one-way analysis of variance with Bonferroni's *post hoc* test. p values of <0.05 were considered statistically significant.

RESULTS

Effects of Asymmetrical Cl^- Removal in Unstimulated Cells—Under control conditions, removal of Cl^- from the apical perfusate did not change pH_i, indicating little resting apical anion exchange (AE) activity (Fig. 1*A*), which would be expected to cause an alkalinization. In marked contrast, basolateral Cl^- removal produced a large, monophasic alkalinization of 0.43 ± 0.01 pH units ($p < 0.001$; $n = 35$). Cl^- readdition reversed this response at an initial rate of 0.52 ± 0.03 pH units/min ($-J(B) = 49.1 \pm 7.0$ mM B min^{-1}). These results indicate functional AE activity in the basolateral, but not apical, membrane of Calu-3 cells under resting conditions, probably mediated by anion exchanger 2 (AE2) (32, 33).

Effects of Cl^- Removal Subsequent to cAMP Elevation—Exposure of cells to forskolin (fsk; 5 μM) under symmetrical high Cl^- conditions significantly acidified pH_i by 0.13 ± 0.01 units (Fig. 1*A*), at a rate of 0.08 ± 0.01 pH units/min. Subsequent apical Cl^- removal markedly alkalinized fsk-treated cells by 0.64 ± 0.03 pH units ($p < 0.001$; $n = 35$; Fig. 1*B*). The pH response was typically biphasic, consisting of a fast initial alkalinization followed by a slower secondary rise in pH_i that reached a steady state after 3–4 min (Fig. 1*A*). Upon Cl^- readdition, pH_i recovered to base-line values at an initial rate of 0.77 ± 0.08 pH units/min ($-J(B) = 67.3 \pm 13.3$ mM B min^{-1}: Fig. 1*B*). Interestingly, under fsk stimulation, removal of basolateral Cl^- produced no change in pH_i (Fig. 1*A*), which indicates that fsk treatment both inhibits basolateral AE and stimulates apical AE activity. Dideoxyforskolin, an inactive analog of fsk, did not mimic these effects, thus confirming that a change in intracellular cAMP provided the fsk-induced "switch" in the Cl^--dependent apical and basolateral pH_i responses ($p > 0.05$ compared with non-stimulated apical and basolateral Cl^--dependent changes in pH_i; $n = 3$; data not shown). Furthermore, both vasoactive intestinal peptide and adenosine, physiological, cAMP-mediated agonists in Calu-3 cells (34, 35), changed pH_i in response to apical Cl^- removal, similar to the fsk-stimulated response ($p > 0.05$; $n = 4$; Fig. 1*C*). Consistent with a cAMP/PKA-dependent activation of an apical AE, the Cl^--dependent pH_i responses were reduced by the PKA inhibitor H-89 as well as by the general PK inhibitor staurosporine (Fig. 1*D*; Calu-3 cells were somewhat insensitive to H-89 and required preincubation at a relatively high concentration (50 μM), which may have PKA-independent effects). The changes in pH_i caused by apical Cl^- removal in fsk-treated cells depended entirely on HCO_3^-; replacement of $NaHCO_3$ with Na-HEPES markedly reduced the Cl^--dependent alkalinization and pH_i recovery (Fig. 1*E*). Finally, and in contrast to the results with cAMP agonists, raising cytosolic Ca^{2+} had no effect

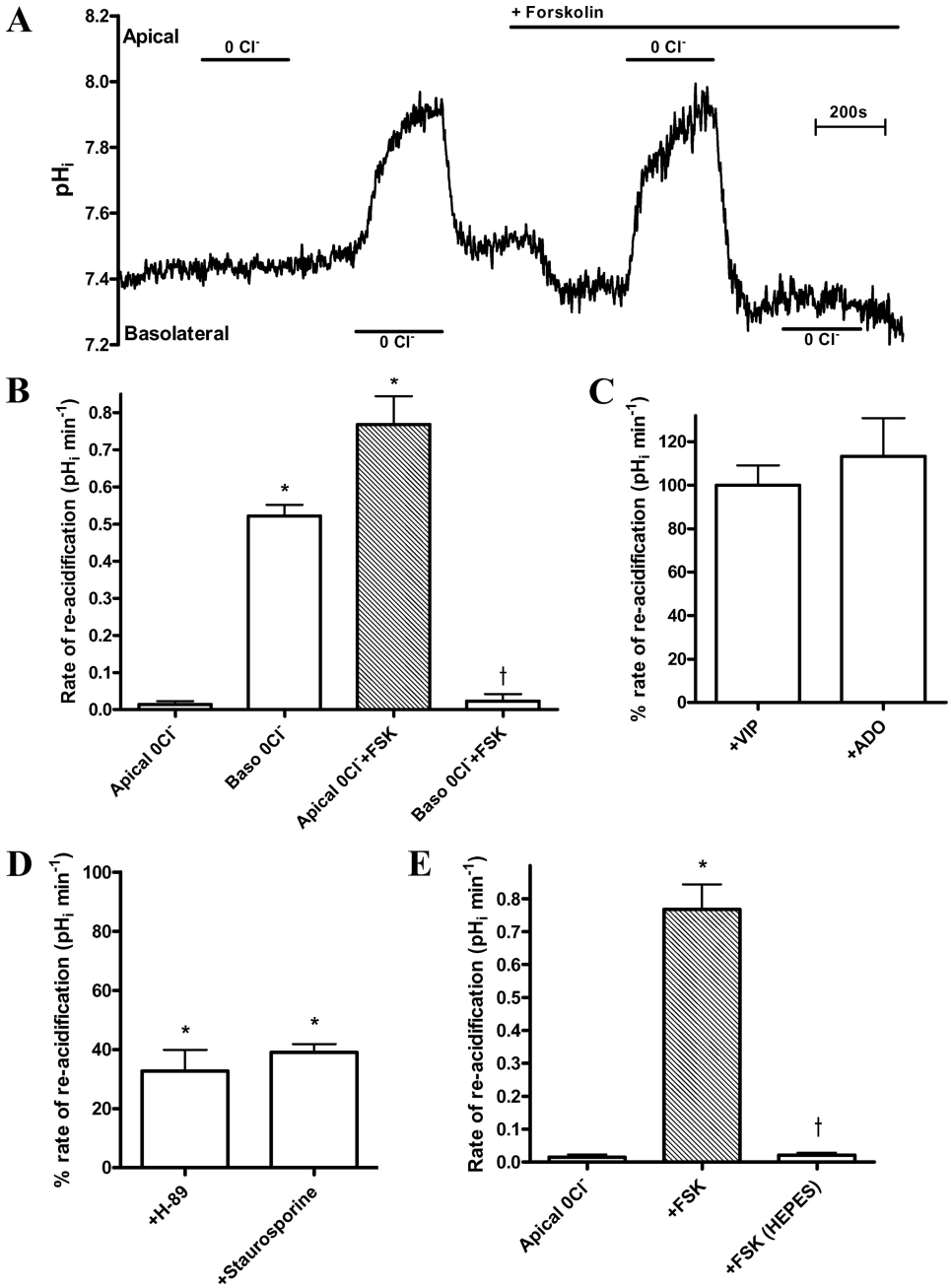

FIGURE 1. **cAMP activates apical Cl^--dependent HCO_3^- transport in polarized cultures of Calu-3 cells.** *A*, representative experimental trace showing the effect of Cl^- removal (*0Cl*$^-$) from the HCO_3^--buffered bathing solution on pH_i in non-stimulated and forskolin-stimulated (*FSK*; 5 μM) conditions. *B*, mean ΔpH_{RA} following apical Cl^- readdition under non-stimulated and fsk-stimulated conditions ($n = 35$; paired observations; *, $p < 0.001$ compared with apical 0Cl^-. †, $p < 0.001$ compared with basolateral 0Cl^-). *C*, the effect of basolateral vasoactive intestinal peptide (*VIP*; 150 nM) and bilateral adenosine (*ADO*; 10 μM) on the ΔpH_{RA} following apical Cl^- readdition. Data are expressed as a percentage of the rate obtained with fsk-treated monolayers ($n = 4$). All agonists performed in parallel using separate monolayers. *D*, effect of H-89 (50 μM) and staurosporine (1 μM) on ΔpH_{RA} following apical Cl^- readdition in fsk-treated Calu-3 cells ($n = 8$). Cell cultures were pretreated with either inhibitor for 60 min. Inhibitors were present in all solutions throughout the experiment. Inhibitor-treated and untreated Calu-3 cells ran in parallel. *, $p < 0.001$ compared with apical 0Cl^- plus forskolin. *E*, effect of external HCO_3^- on mean ΔpH_{RA} following apical Cl^- readdition in fsk-stimulated Calu-3 cells. HCO_3^--free solutions were buffered to pH 7.4 with NaHEPES ($n = 5$; paired observations; *, $p < 0.001$ compared with apical 0Cl^-; †, $p < 0.001$ compared with apical 0Cl^- plus forskolin). *Error bars*, S.E.

on apical AE activity (supplemental Fig. S1). Taken together, these results suggest that the observed changes in pH_i are due to cAMP/PKA activation of an apical Cl^--dependent HCO_3^- transporter, which strongly selects for HCO_3^- over OH^-.

Properties of cAMP-stimulated Responses to Apical Cl^- Removal—The ability of different anions to support reacidification following Cl^- withdrawal was next measured. Recovery of pH_i was supported by a range of monovalent but not divalent anions. A clear selectivity exists among the monovalent anions, with I^- and Br^- exhibiting the highest rate of reacidification compared with the other anions ($p < 0.01$; $n = 5$). The anion/Cl^- selectivity ratio sequence was as follows: $HCOO^-$, 0.6; NO_3^-, 0.8; SCN^-, 0.8; Cl^-, 1; Br^-, 1; I^-, 1.3 (Fig. 2*A*). Removal of Na^+ had no significant effect on the rate of reacidification (ΔpH_{RA}) ($p > 0.05$; $n = 4$; Fig. 2*B*). Similarly, hyperpolarization of the resting membrane potential (V_m) using the K^+ channel

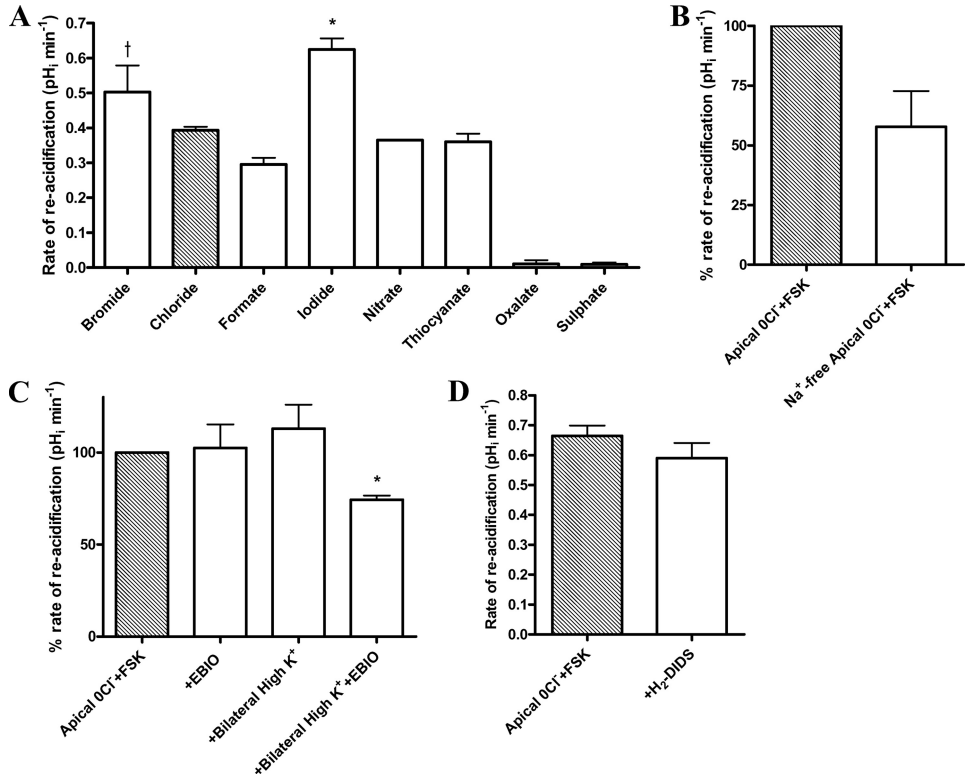

FIGURE 2. **Ionic dependence of apical Cl^--dependent HCO_3^- transport in forskolin-stimulated Calu-3 cell monolayers.** *A*, anion selectivity of the apical Cl^--dependent pH_i changes measured by the ability of the replacement anion (for Cl^-) to support reacidification under fsk-stimulated conditions. Anions were added iso-osmotically to replace Cl^-. ($n = 5$; paired observations; *, $p < 0.01$ compared with chloride; †, $p < 0.001$ compared with formate, nitrate, and thiocyanate). *B*, the effect of bilateral Na^+ removal on ΔpH_{RA} upon apical Cl^- readdition in fsk-treated cells. Data are expressed as a percentage of the rate obtained with fsk-treated monolayers in the presence of bilateral Na^+ ($n = 4$; Na^+-containing and Na^+-free Krebs solutions applied in separate experiments, performed in parallel). *C*, the effect of bilateral high K^+ (115 mM) and K^+ channel opener EBIO (1 mM) on the percentage ΔpH_{RA} upon apical Cl^- readdition in fsk-stimulated cells. Shown are pH_i responses in high K^+ and EBIO compared with control apical $0Cl^-$ plus forskolin (*FSK*) responses. Each condition was measured in separate experiments performed in parallel ($n = 4$; *, $p < 0.05$ compared with apical $0Cl^-$ plus forskolin). *D*, the effect of apical H_2-DIDS (500 μM) on the ΔpH_{RA} upon apical Cl^- readdition in fsk-stimulated cells ($n = 4$; paired observations). *Error bars*, S.E.

opener 1-ethyl-2-benzimidazolinone (EBIO; 1 mM) likewise was without effect (Fig. 2*C*). However, clamping V_m to 0 mV through a combination of high extracellular K^+ plus EBIO did reduce the rate of reacidification by 23.7 ± 2.3% ($p < 0.05$; $n = 4$; Fig. 2*C*), indicating some dependence on V_m. The ΔpH_{RA} was also insensitive to the general anion transport inhibitor 4,4′-diisothiocyano-1,2-diphenylethane-2,2′-disulfonate (H_2-DIDS) ($p > 0.05$; $n = 4$; Fig. 2*D*). The observed changes in pH_i depicted in Figs. 1 and 2 are therefore due to the activity of a Na^+-independent, H_2-DIDS-insensitive, electrogenic, monovalent anion transporter, consistent with the known properties of CFTR.

Contribution of CFTR and Basolateral Cl^-/HCO_3^- Exchange to pH_i Responses—To determine whether CFTR contributes to the alkalinization caused by apical Cl^- removal, the effect of CFTR inhibition was tested. GlyH-101 (10 μM) abolished the pH_i response to apical Cl^- removal in fsk-stimulated Calu-3 monolayers (lack of alkalinization in the presence of GlyH-101, shown by the *black trace* in Fig. 3*A*). $CFTR_{inh}$-172 produced similar results (10 μM) (data not shown). Note that the initial exposure to GlyH-101 caused an alkalinization that is probably due to inhibition of HCO_3^- efflux from the cells.

In the absence of a CFTR blocker, the activity of a basolateral H_2-DIDS-sensitive "base" transporter strongly influenced both the magnitude of the pH_i response to apical Cl^- removal and the ΔpH_{RA} (supplemental Fig. S2). To ascertain whether a basolateral H_2-DIDS-sensitive transporter also affects the Cl^--dependent pH_i response in the presence of GlyH-101, Calu-3 monolayers were first exposed to basolateral H_2-DIDS *before* GlyH-101. This maneuver restored apical Cl^--induced pH_i changes to GlyH-101-treated cells (Fig. 3*A*, *blue trace*) and indicated the presence of an apical Cl^-/HCO_3^- exchanger. In contrast to the rates of alkalinization with Cl^- removal, the ΔpH_{RA} upon apical Cl^- readdition was significantly reduced under these conditions ($p < 0.001$; $n = 4$; Fig. 3*C*). These data suggest that apical Cl^-/HCO_3^- exchange is functionally coupled to Cl^- transport by CFTR or that CFTR itself directly contributes to pH changes, in addition to the exchanger.

Knockdown of CFTR Provides Additional Evidence for a Role of both CFTR and a Coupled Anion Exchanger— The role of CFTR in regulating apical Cl^-/HCO_3^- exchange was next investigated using CFTR KD Calu-3 cells (29). CFTR content of KD cells was determined to be ~28 ± 5% that of wild-type (WT) cells (supplemental Fig. S3, *A* and *B*). Compared with WT cells, cAMP-stimulated secretory capacity in these CFTR KD cells was also reduced by ~25% (29). Mean pH_i values did not differ significantly between WT (7.43 ± 0.03; $n = 50$) and CFTR KD (7.39 ± 0.05; $n = 32$; $p > 0.05$) Calu-3 cells. The switch from basolateral to apical AE activity in response to cAMP is preserved in CFTR KD cells (Fig. 4*A*). However, in CFTR KD cells,

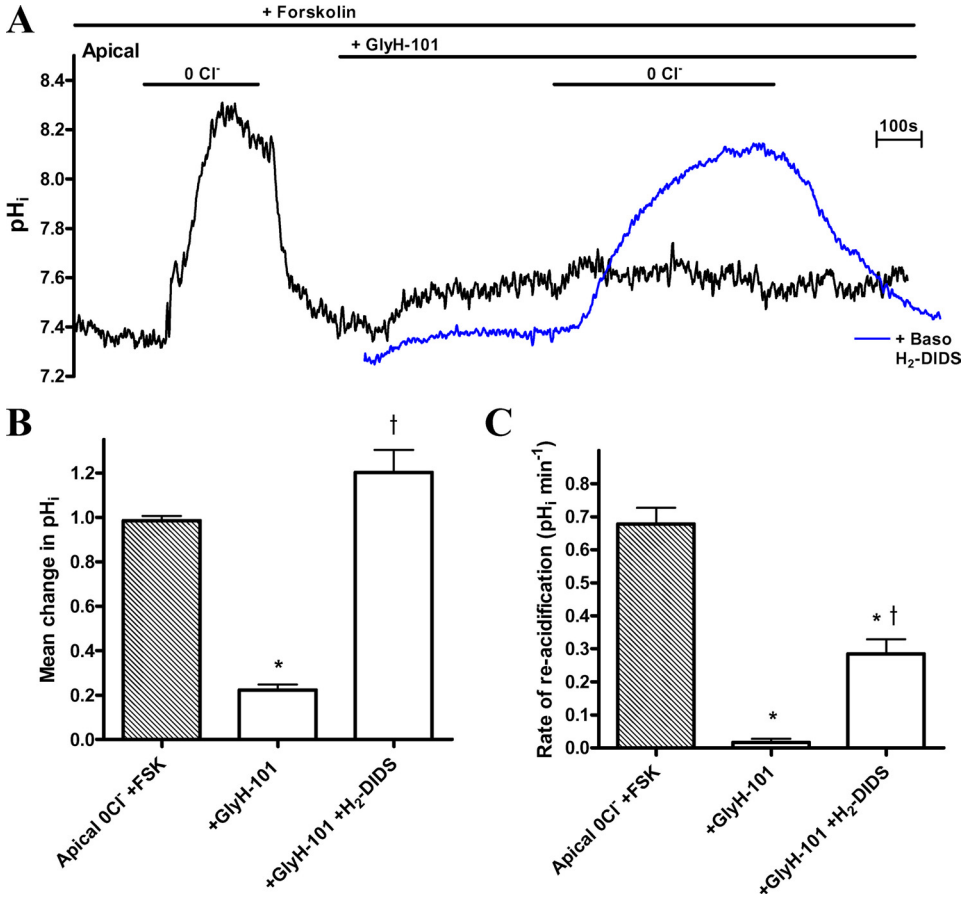

FIGURE 3. **Demonstration of apical Cl^-/HCO_3^- exchange activity in the presence of apical GlyH-101 solely or in combination with basolateral H_2-DIDS.** *A*, experimental traces of the effect of apical GlyH-101 (10 μM) on apical Cl^--induced changes in pH_i in fsk-stimulated (5 μM) Calu-3 cells, in the presence (*blue trace*) and absence (*black trace*) of basolateral H_2-DIDS (500 μM). *B*, the mean change in pH_i produced by apical Cl^- removal under each condition ($n = 4$; *, $p <$ 0.001 compared with apical 0Cl^- plus forskolin (*FSK*); †, $p < 0.01$ compared with +GlyH-101). *C*, the ΔpH_{RA} upon apical Cl^- readdition under each condition ($n = 4$; paired observations; *, $p < 0.001$ compared with apical 0Cl^- plus forskolin; †, $p < 0.01$ compared with +GlyH-101). *Error bars*, S.E.

the basolateral anion exchanger was not fully inhibited under fsk-stimulated conditions (compare Figs. 1*A* and 4*A*). The reduced expression of CFTR in the CFTR KD Calu-3 cells was reflected in a reduced ΔpH_{RA} (~48%), which decreased from 0.75 ± 0.09 pH units/min ($-J(B) = 97.6 \pm 13.3$ mM B min^{-1}) in WT cells to 0.39 ± 0.02 pH units min^{-1} ($-J(B) = 65.9 \pm 9.8$ mM B min^{-1}) in KD cells ($p < 0.01$; $n = 4$; Fig. 4*B*). These values are similar to those obtained in GlyH-101/H_2-DIDS-treated WT Calu-3 cells (Fig. 3*B*). Although ΔpH_{RA} was slower, the profile of the apical Cl^--dependent change in pH_i in CFTR KD Calu-3 monolayers broadly resembled that of WT cells, being H_2-DIDS-insensitive, abolished by GlyH-101 addition in the absence of basolateral H_2-DIDS (data not shown), and supported only by monovalent anions. However, the I^-/Cl^- selectivity ratio significantly increased from 1.3 in WT cells to 2.1 in CFTR KD cells ($p < 0.001$; $n = 4$; Fig. 4*C*; see "Discussion"). Taken together, these results suggest that both CFTR and an apical Cl^-/HCO_3^- exchanger contribute to Cl^--induced pH_i changes in Calu-3 cells.

Pendrin Is Expressed in Calu-3 and Human Airway Cells—Apical SLC26A family Cl^-/HCO_3^- exchangers contribute to transepithelial HCO_3^- secretion in other HCO_3^--secreting epithelia. To identify the apical AE, quantitative RT-PCR was performed for all 10 members of the *SLC26A* family (36) using RNA extracted from polarized Calu-3 cells. Fig. 5*A* shows that a number of SLC26A transporters are expressed in Calu-3 cells, several of which are known to function as Cl^-/HCO_3^- exchangers (SLC26A4, -A6, -A7, and -A9). Of these four candidates, only pendrin (SLC26A4) has properties that are consistent with our results: a monovalent anion transporter with high affinity for iodide and insensitivity to H_2-DIDS (37–40). A mouse polyclonal anti-SLC26A4 antibody detected a band migrating at ~100 kDa in immunoblot analysis of Calu-3 whole cell lysates (supplemental Fig. S4). The size of the detected species is consistent with that of the band detected using heterologously expressed pendrin fusion proteins as well as with previous reports (41). Confocal immunofluorescence images revealed a punctate localization of pendrin near the apical membrane of Calu-3 monolayers (Fig. 5*C*, *top*, *green*), when compared with ZO-1 expression (Fig. 5*C*, *bottom*, *red*). Immunohistochemical studies on native human tissue showed that pendrin is highly expressed in surface ciliated cells, is not present in mucous-secreting cells of submucosal glands, and is present, albeit at a lower level than in ciliated cells, in serous-like cells from SMGs (supplemental Fig. S5). This work provides additional support for pendrin expression in human airway serous cells and also confirms that pendrin is expressed in surface bronchial epithelial cells (42).

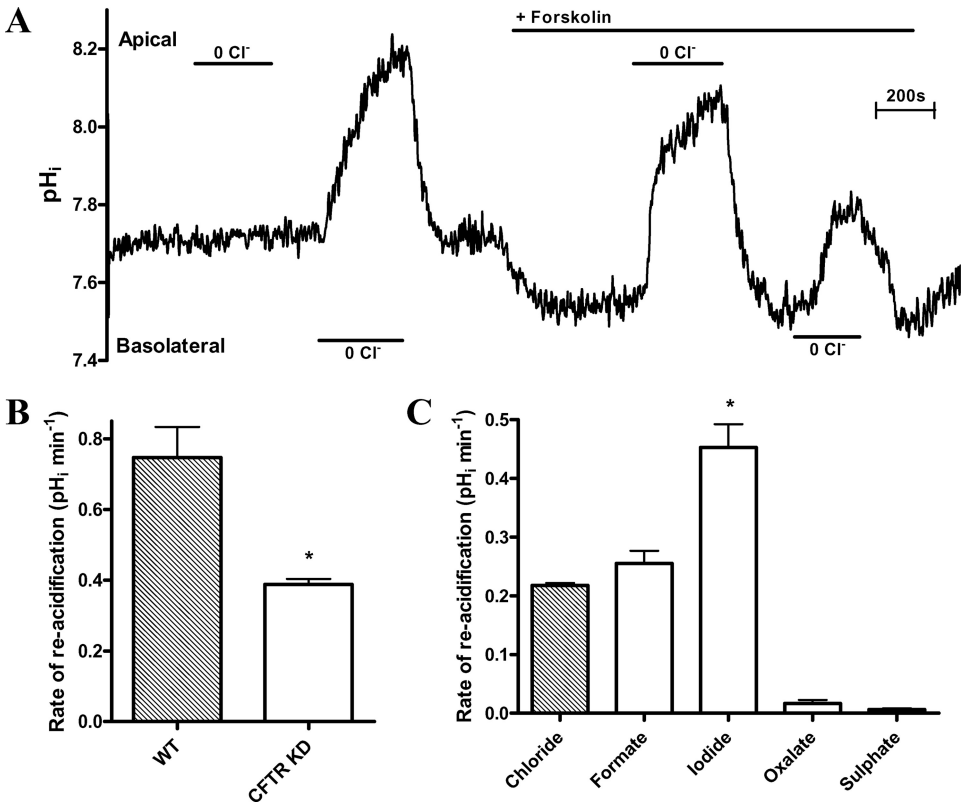

FIGURE 4. **Apical Cl^--dependent HCO_3^- transport in Calu-3 cells is partially CFTR-dependent.** *A*, trace showing the effect of Cl^- removal ($0Cl^-$) on pH_i under non-stimulated and fsk-stimulated (*FSK*; 5 μM) conditions in CFTR KD Calu-3 cells. *B*, comparison of the mean ΔpH_{RA} upon apical Cl^- readdition in WT and CFTR KD Calu-3 cells. WT and CFTR KD experiments carried out in parallel ($n = 4$; *, $p < 0.01$ compared with WT). *C*, the mean rate of pH_i recovery in CFTR KD Calu-3 cells upon introduction of monovalent (chloride, formate, and iodide) and divalent (oxalate and sulphate) anions following apical Cl^- removal under fsk-stimulated conditions. Anions were added iso-osmotically to replace Cl^- ($n = 4$; paired observations; *, $p < 0.001$ compared with chloride and formate). *Error bars*, S.E.

Pendrin Knockdown Provides Insights into Its Function in Calu-3 Cells—To establish if pendrin functions in HCO_3^- transport in Calu-3 cells, pendrin (SLC26A4) and cyclophilin B (control) KD Calu-3 cells were produced by shRNA inhibition. Knockdown was verified using both quantitative RT-PCR and immunodetection methods. Pendrin mRNA expression in these KD cells was reduced to 8.5 ± 0.7% compared with cyclophilin B (control) KD Calu-3 cells ($p < 0.05$; $n = 3$; Fig. 5*B*). Confocal immunofluorescence imaging verified pendrin expression in both control KD Calu-3 monolayers and CFTR KD Calu-3 cells, whereas no signal was detected in the pendrin KD cells (Fig. 5*C*).

Although pendrin KD cells showed a fsk-stimulated apical Cl^--dependent change in pH_i, the ΔpH_{RA} was reduced by 47.6 ± 2.4%, compared with control KD cells ($p < 0.001$; $n = 5$; Fig. 5*D*). Like CFTR KD cells, the profile of the apical Cl^--dependent change in pH_i in pendrin KD cells was reminiscent of WT Calu-3 cells. It was only supported by monovalent anions (Fig. 5*E*), was H_2-DIDS-insensitive (Fig. 5*F*), and was abolished by GlyH-101 addition (data not shown). Interestingly, unlike WT as well as CFTR KD cells, the pendrin KD cells showed no significant difference in the ΔpH_{RA} when iodide replaced chloride ($p > 0.05$; $n = 4$; Fig. 5*E*). This observation is consistent with the KD of an AE which has a high affinity for iodide. Neither pendrin nor control KD Calu-3 cells showed significant differences in CFTR protein expression ($p > 0.05$; $n = 3$; supplemental Fig. S3, *A* and *B*). Thus, these differences in apical Cl^--induced changes in pH_i in pendrin KD cells do not reflect a change in CFTR expression. In addition, short circuit current (I_{SC}) measurements demonstrated a similar GlyH-101-sensitive fraction of fsk-stimulated I_{SC} (indicative of CFTR-dependent anion transport) in pendrin and control KD Calu-3 monolayers ($p > 0.05$; $n = 9$; supplemental Fig. S3*C*). The H_2-DIDS insensitivity of the apical Cl^--dependent changes in pH_i in WT and pendrin KD Calu-3 cells suggests that other SLC26 members highly expressed in these cells, such as SLC26A2 or SLC26A6 (both are sensitive to H_2-DIDS (43, 44)), are unlikely to be involved in these responses.

pH_i Response to Cl^- Removal by Fisher Rat Thyroid Cells Expressing CFTR or Pendrin—The significant changes in I^-/Cl^- ratio for the ΔpH_{RA} across the different cell types (Figs. 2*A*, 4*C*, and 5*E*), together with expression data and pharmacological responses to H_2-DIDS and GlyH-101, indicate that both CFTR and pendrin contribute to the Cl^--induced pH_i responses. As a further test, the pH_i responses to Cl^- removal and readdition were evaluated in polarized FRT monolayers stably expressing either CFTR or pendrin alone (30). Fig. 6*A* shows that FRT cells expressing CFTR alkalinized in response to apical Cl^- removal in the presence of fsk, supporting the notion that CFTR can conduct HCO_3^- *into* the cell under an imposed outwardly directed Cl^- gradient. The pH_i response to apical Cl^- was significantly augmented after fsk treatment.

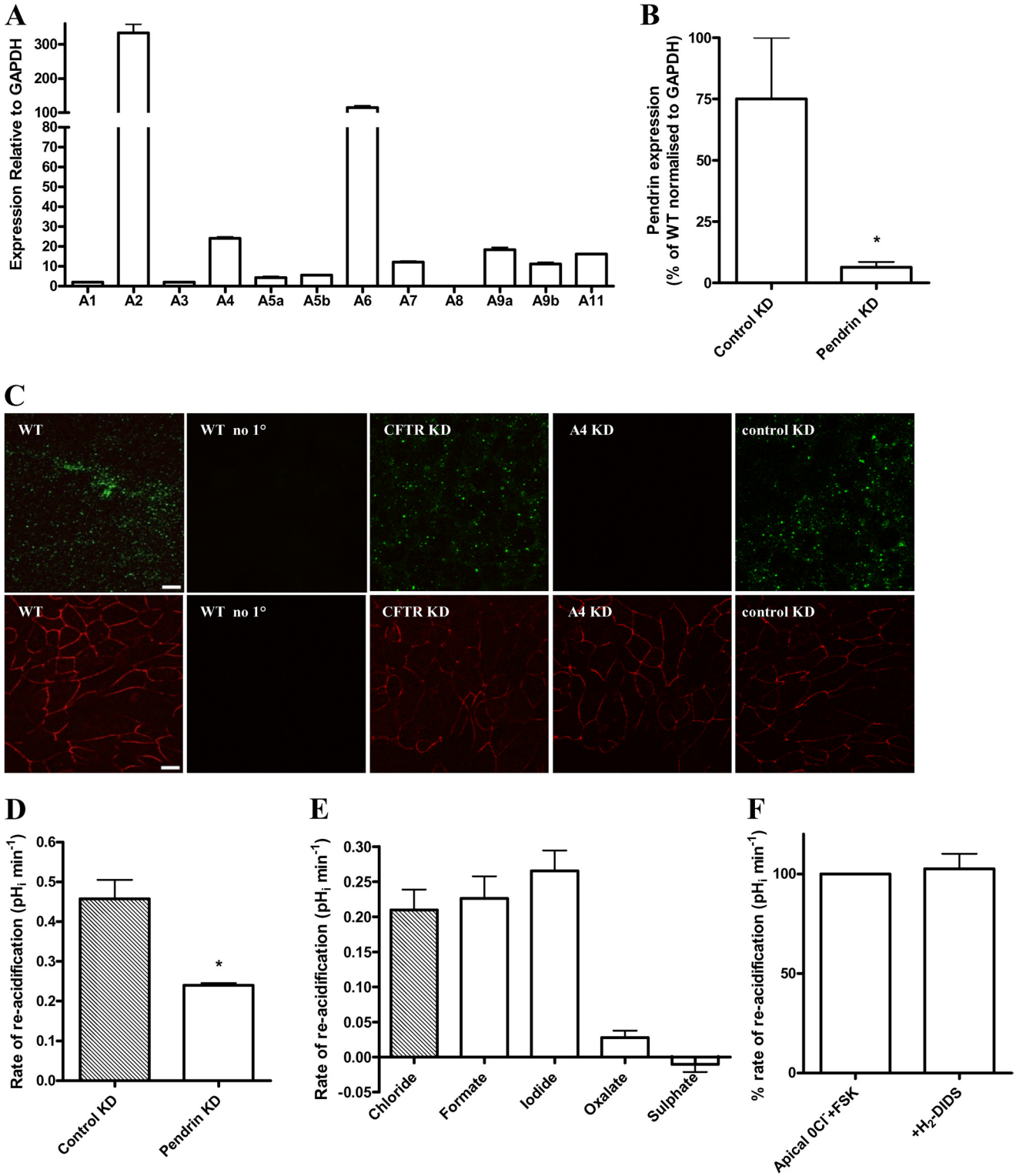

FIGURE 5. **Pendrin knockdown Calu-3 cells show reduced apical Cl^--dependent HCO_3^- transport.** *A*, quantitative RT-PCR (Taqman) analysis of *SLC26* mRNA expression in WT Calu-3 cells grown on Transwell supports, relative to standard curve and normalized to *GAPDH* (%) ($n = 3$ separate cell cultures). *B*, quantitative RT-PCR analysis of the percentage of pendrin expression in pendrin KD Calu-3 cells normalized to GAPDH compared with that of cyclophilin B KD (*Control KD*) Calu-3 cells ($n = 3$). *C*, confocal micrographs showing pendrin (*green*; *upper panels*) and ZO-1 (*red*; *lower panels*) staining in wild type (*WT*), CFTR knockdown (*CFTR KD*), pendrin KD (*A4 KD*), and cyclophilin B KD (*control KD*) Calu-3 cell monolayers. *WT no 1°*, immunofluorescence from WT Calu-3 cells with only the secondary antibodies applied. Note that cells treated with either antibody are separate *xy* sections taken from the same confluent monolayer of each cell type, and images were acquired under identical conditions of illumination intensity and photomultiplier settings. *Scale bars*, 10 μm ($n = 3$). *D*, comparison of the mean ΔpH_{RA} upon readdition of Cl^- in cyclophilin B (control) KD and pendrin KD Calu-3 cells. Control KD and pendrin KD cell experiments were carried out in parallel. ($n = 5$; *, $p < 0.001$ compared with control KD). *E*, the mean ΔpH_{RA} in pendrin KD Calu-3 cells upon introduction of monovalent (chloride, formate, and iodide) and divalent (oxalate and sulfate) anions following apical Cl^- removal under fsk-stimulated conditions ($n = 4$; paired observations). *F*, the effect of apical H_2-DIDS (500 μM) on the ΔpH_{RA} upon apical Cl^- readdition in fsk-stimulated pendrin KD cells. Data expressed as a percentage of the rate obtained with control fsk-treated monolayers ($n = 4$; paired observations). *Error bars*, S.E.

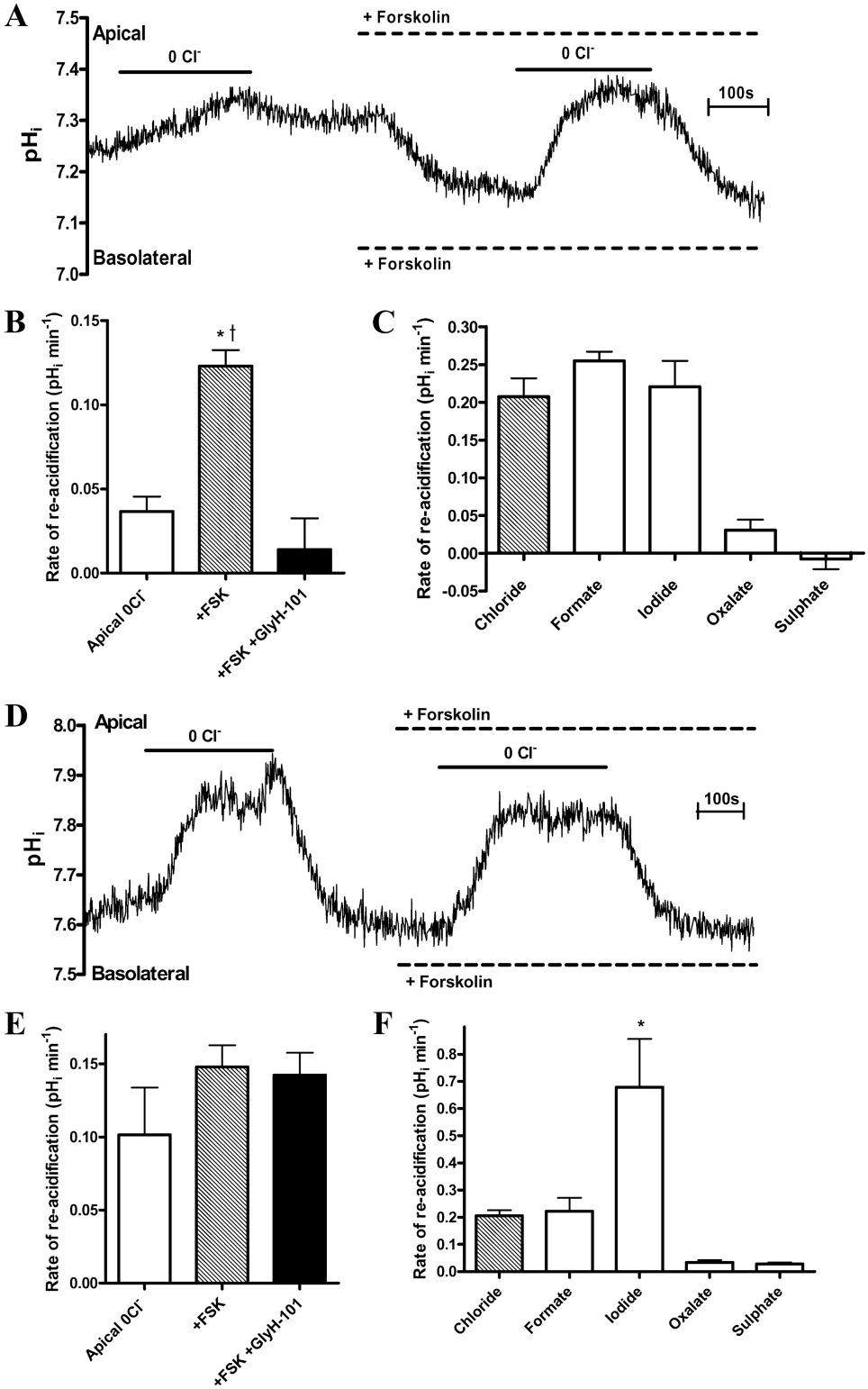

FIGURE 6. **Properties of Cl^--dependent changes in pH_i in CFTR- and pendrin-transfected FRT cells.** *A* and *D*, experimental traces showing the effect of forskolin (5 μM) on changes in pH_i following the removal of apical Cl^- in CFTR-transfected (*A*) and pendrin-transfected (*D*) FRT cell monolayers. Note that untransfected FRT cells produced no response to this maneuver (data not shown). *B* and *E*, the effect of fsk and fsk plus GlyH-101 (10 μM) on ΔpH_{RA} following apical Cl^- readdition in CFTR-transfected (*B*) and pendrin-transfected (*E*) FRT cells ($n = 4$; paired observations; *, $p < 0.05$ compared with apical $0Cl^-$. †, $p < 0.01$ compared with +forskolin and GlyH-101). *C* and *F*, the mean ΔpH_{RA} produced by the introduction of monovalent (iodide, formate, and chloride) and divalent (oxalate and sulfate) anions following the removal of apical Cl^- in CFTR-transfected (*C*) and pendrin-transfected (*F*) FRT cells ($n = 4$; paired observations; *, $p <$ 0.05 compared with Cl^- and formate). *Error bars*, S.E.

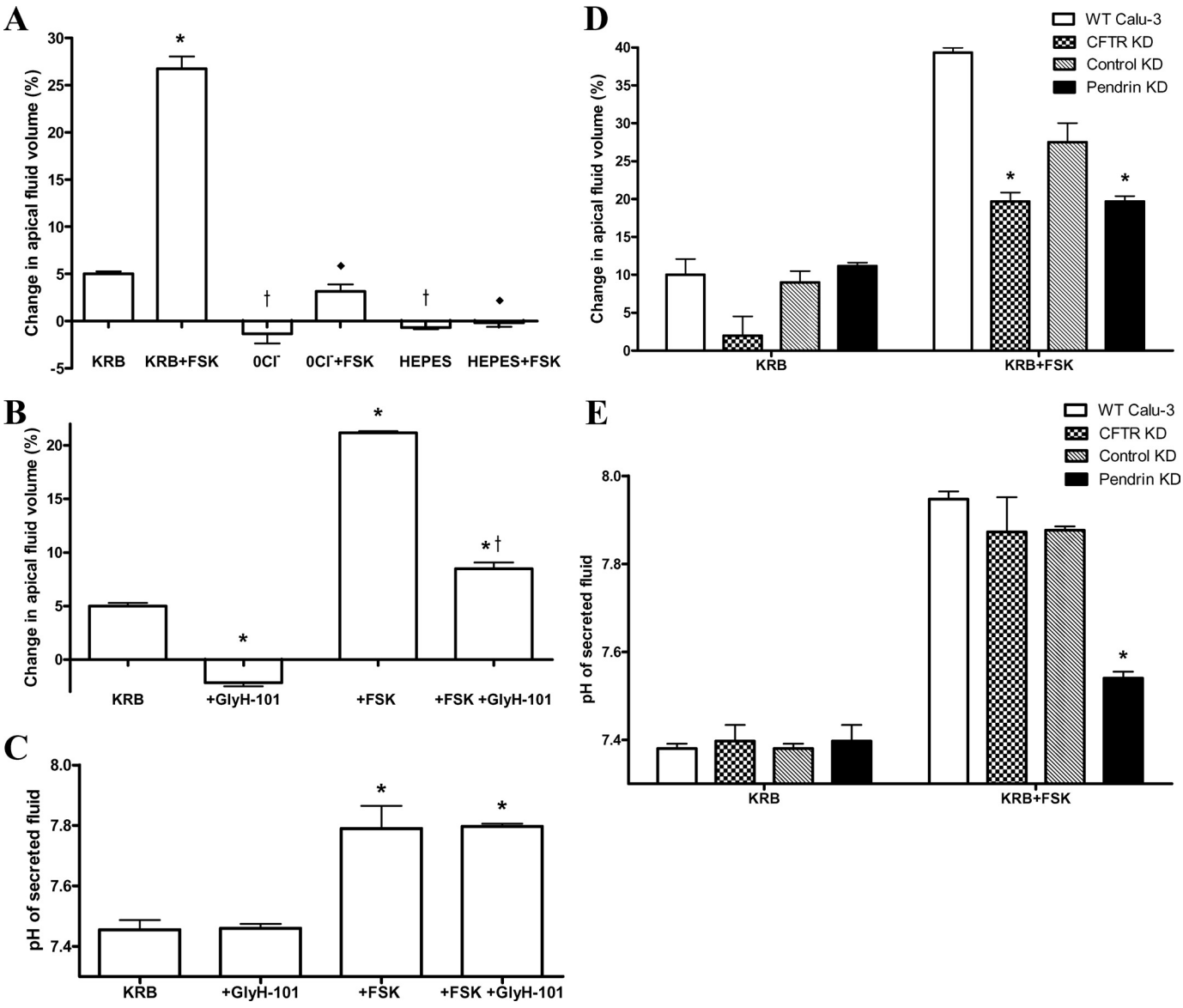

FIGURE 7. **Assessment of transepithelial fluid secretion rates and fluid pH.** *A*, changes in the rate of transepithelial fluid secretion by wild-type Calu-3 cell monolayers in response to bilateral Cl^- and HCO_3^- removal, using Cl^--free HCO_3^--buffered (*0Cl*$^-$) and HEPES-buffered Krebs (*HEPES*) solutions under non-stimulated and forskolin-stimulated (*FSK*) conditions, compared with liquid secretion from monolayers bathed in the standard KRB. Forskolin (5 μM) was applied to both the apical and basolateral solutions. Rates were calculated based on 24-h fluid accumulation volumes. Changes in apical fluid volume are expressed as a percentage compared with the starting volume of 200 μl ($n = 6$; *, $p < 0.001$ compared with KRB; †, $p < 0.01$ compared with KRB; ♦, $p < 0.001$ compared with KRB plus forskolin). *B*, the effect of CFTR inhibition by GlyH-101 (10 μM) on the rate of apical liquid secretion (percentage change in volume) from non-stimulated and fsk-stimulated wild type Calu-3 cell monolayers over 24 h ($n = 3$; *, $p < 0.001$ compared with KRB; †, $p < 0.001$ compared with forskolin-stimulated conditions). *C*, the effect of CFTR inhibition by GlyH-101 (10 μM) on the pH of the apical liquid secreted from non-stimulated and fsk-stimulated wild type Calu-3 cell monolayers over 24 h ($n = 3$; *, $p < 0.001$ compared with KRB and KRB + GlyH-101). Fluid volume and pH measurements represent paired observations from the same Transwells. *D*, comparison of the rates of apical fluid secretion (percentage change in volume) by all four Calu-3 lines evaluated in this study, under non-stimulated and fsk-stimulated conditions. Data from wild-type, CFTR KD, cyclophilin B knockdown (*control KD*), and pendrin knockdown (*A4 KD*) Calu-3 cell monolayers are shown. Percentage changes were calculated from the accumulated volumes over 24 h ($n = 3$; *, $p < 0.05$ compared with control KD plus forskolin). *E*, pH of apical fluid secreted from non-stimulated and fsk-stimulated wild-type, CFTR KD, cyclophilin B knockdown (*control KD*), and pendrin knockdown (*A4 KD*) Calu-3 cell monolayers over 24 h ($n = 3$; *, $p < 0.01$ compared with control KD plus forskolin). Fluid volume and pH measurements represent paired observations from the same Transwells. *Error bars*, S.E.

This increase could be completely inhibited by GlyH-101; thus, CFTR mediated the changes in pH_i (Fig. 6, *A* and *B*). Anion substitution studies revealed that only monovalent anions supported reacidification, and I^- and Cl^- selectivity did not differ (Fig. 6*C*). Pendrin-expressing FRT cells responded to apical Cl^- removal very differently. Significant Cl^--induced pH_i responses were observed in the absence of cAMP stimulation (Fig. 6*D*). This Cl^-/HCO_3^- AE activity was not enhanced by fsk or inhibited by GlyH-101 (Fig. 6, *D* and *E*). Importantly, the ΔpH_{RA} was markedly higher for I^- compared with Cl^- (Fig. 6*F*; $I^-/Cl^- = 3.2$), with no ability to transport divalent anions, results that are entirely consistent for pendrin (39, 40).

Anion Transport Is Critical for Fluid Secretion—We next measured and compared both the rate of transepithelial liquid secretion (J_v) and the pH of secreted fluid samples from WT, CFTR KD, and pendrin KD monolayers. WT Calu-3 monolay-

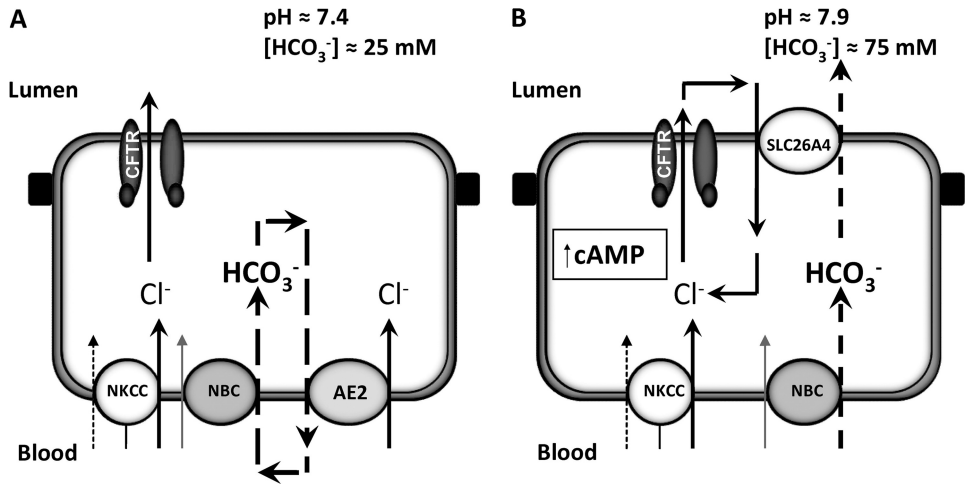

FIGURE 8. **Proposed model for HCO_3^- secretion in human airway serous cells.** *A* and *B*, diagram illustrating the movement of Cl^- and HCO_3^- ions across the basolateral and luminal membrane of non-stimulated (*A*) and cAMP-stimulated (*B*) Calu-3 cells, based on pH_i and transepithelial fluid secretion studies. Under non-stimulated conditions, Cl^- is accumulated across the basolateral membrane by the combined action of the basolateral Na^+-K^+-$2Cl^-$ cotransporter, NKCC1, together with parallel activity of the NBC and AE2 (32, 33). Under these conditions, a basal level of CFTR activity drives a small amount of a Cl^--rich secretion with a pH of ~7.4 (25 mM HCO_3^-) via electrogenic Cl^- efflux through CFTR. Elevation of cAMP inhibits basolateral AE2 and stimulates NBC (21). At the apical membrane, cAMP/PKA further increases CFTR activity as well as activates pendrin (SLC26A4). Stimulation of CFTR activity leads to a marked rise in net transepithelial fluid secretion driven by electrogenic Cl^- efflux through CFTR, whereas the co-activation of pendrin increases the HCO_3^- content of this secreted fluid to ~75 mM (pH 7.9), through coupled Cl^-/HCO_3^- exchange, with Cl^- cycling across the apical membrane via CFTR and SLC26A4.

ers, submerged in HCO_3^--KRB, increased the apical fluid volume from 200 μl to 210 ± 1 μl over 24 h ($p < 0.05$; $n = 6$; Fig. 7*A*), corresponding to a J_v of 0.42 ± 0.02 μl/cm^2/h. Forskolin increased J_v ~5-fold to 2.23 ± 0.11 μl/cm^2/h ($p < 0.001$; $n = 6$). Bilateral Cl^- removal abolished basal liquid secretion and reduced fsk-stimulated secretion by 88 ± 22% ($p < 0.001$; $n = 6$). No significant fluid secretion was observed from Calu-3 monolayers bathed in HEPES-buffered KRB under either non-stimulated or fsk-stimulated conditions ($p > 0.05$; $n = 6$). These results show that both basal and fsk-stimulated Calu-3 liquid secretion are entirely Cl^-- and HCO_3^--dependent.

To determine the role played by CFTR in transepithelial HCO_3^- and liquid secretion, experiments were performed with the CFTR blocker, GlyH-101. In the presence of apical GlyH-101, non-stimulated WT Calu-3 cells absorbed rather than secreted fluid (−0.18 ± 0.01 μl/cm^2/h; $p < 0.001$; $n = 3$; Fig. 7*B*), suggesting that all basal liquid secretion involves CFTR. Forskolin-stimulated fluid secretion was substantially inhibited by GlyH-101 (60 ± 7% inhibition; $p < 0.001$; $n = 3$) but nonetheless achieved levels significantly greater than control ($p < 0.001$; $n = 3$). Assuming complete block of CFTR in these experiments, these results suggest that although the majority of the cAMP-stimulated liquid secretion depends on CFTR, a significant CFTR-independent, cAMP-stimulated, component of liquid secretion does exist. The pH of the apical fluid from non-stimulated Calu-3 monolayers did not differ significantly from that of the bathing Krebs solution (compared with pH 7.4; $p > 0.05$; $n = 3$; Fig. 7*C*). However, apical fluid pH significantly increased to 7.8 ± 0.1 (~60 mM HCO_3^-) following fsk stimulation ($p < 0.001$; $n = 3$). Surprisingly, despite reducing the rate of liquid secretion, GlyH-101 addition had no effect on the pH of the secreted fluid under either non-stimulated or forskolin-stimulated conditions ($p > 0.05$; $n = 3$).

The CFTR dependence of Calu-3 liquid secretion was further explored using CFTR KD Calu-3 cells. Under non-stimulated conditions, CFTR KD Calu-3 cells failed to increase the volume of apical fluid over 24 h ($p > 0.05$; $n = 4$; Fig. 7*D*) and secreted significantly less liquid compared with WT cells under fsk-stimulated conditions (34 ± 3% compared with WT; $p < 0.001$; $n = 4$). Like GlyH-101 addition in WT Calu-3 cells, CFTR KD had no significant effect on the pH of secreted apical fluid under either non-stimulated or fsk-stimulated conditions ($p > 0.05$; $n = 3$; Fig. 7*E*). These results establish a critical role for CFTR in regulating the rate of transepithelial liquid secretion but not in controlling the pH ($[HCO_3^-]$) of the secreted fluid.

In contrast, pendrin KD did not significantly affect either the rate of transepithelial liquid secretion or the pH of secreted fluid under basal conditions, compared with control KD Calu-3 cells ($p > 0.05$; $n = 3$; Fig. 7, *D* and *E*). However, although pendrin KD Calu-3 cells produced an increase in fluid volume ($p < 0.05$; $n = 3$) and pH ($p < 0.01$; $n = 3$) in response to fsk addition, comparatively less fluid was secreted ($p < 0.05$; $n = 3$; Fig. 7*D*). Importantly, the secreted fluid was markedly less alkaline (pH 7.54 ± 0.01; $p < 0.001$; $n = 3$; Fig. 7*E*). Taken together, these results are consistent with pendrin mediating the majority of HCO_3^- secretion (exit) across the luminal membrane of Calu-3 monolayers via coupled Cl^-/HCO_3^- exchange. Furthermore, because the osmolarity of the secreted fluid from all treatment groups did not significantly differ from the Krebs buffer (data not shown), any increase in $[HCO_3^-]$ indicates that the $[Cl^-]$ of the secreted fluid must decrease proportionally to maintain constant osmolarity. From the $[Cl^-]$ and volume of fluid secreted, it is possible to estimate total Cl^- secretion capacity for the different cell types (supplemental Table S3). The results show that CFTR KD substantially reduced whereas pendrin KD increased total Cl^- secretion, as would be predicted from their proposed roles in transepithelial salt and fluid secretion in Calu-3 cells (see Fig. 8).

DISCUSSION

Our findings demonstrate for the first time the presence of an apical Cl^-/HCO_3^- exchange activity in cAMP-stimulated Calu-3 cells. This cAMP-activated apical AE activity is Na^+-independent, H_2-DIDS-insensitive, and capable of transporting a broad range of monovalent, but not divalent, anions in exchange for HCO_3^-. The selectivity profile is I = Br > Cl = HCOO = NO_3 = SCN ≫ OH, consistent with pendrin-mediated transport (38, 45). Our results agree with data from *Xenopus* oocytes expressing human SLC26A4, which show that pendrin can function as a Cl^-/HCO_3^- exchanger as well a Cl^-/I^- exchanger (39). Furthermore, mouse parotid duct cells show forskolin-stimulated I^- secretion, which was absent in *Slc26a4*$^{-/-}$ mice (40).

We measured active apical AE activity in cAMP-stimulated cells exposed to no Cl^- ($0Cl^-$) even in the presence of the CFTR inhibitor GlyH-101 (Fig. 3). This strongly suggests that apical HCO_3^- transport can occur independently of CFTR, contrary to many previous Calu-3/SMG studies (17–19, 46, 47). However, in CFTR-transfected FRT cells, apical Cl^- removal also increased pH_i. This was completely GlyH-101-sensitive, indicating that HCO_3^- influx through CFTR does occur under $0Cl^-$ conditions (Fig. 6, *A* and *B*). Therefore, the changes in pH_i following removal of luminal Cl^- in cAMP-stimulated Calu-3 cells could also be interpreted as being due to HCO_3^- influx through CFTR alone or in conjunction with a Cl^-/HCO_3^- exchanger. We favor the latter possibility based on the monovalent anion selectivity, particularly to I^-, of the pH_i response in the different cell types studied. In WT Calu-3 cells, the rate of HCO_3^--dependent reacidification displayed an anion selectivity of I > Cl = HCOO, consistent with the high selectivity of pendrin for I^- (validated in pendrin-transfected FRT cells; Fig. 6*F*). In contrast, CFTR-transfected cells transported each of these monovalent anions at equal rates (Fig. 6*C*). Furthermore, CFTR knockdown in Calu-3 cells (Fig. 4*C*) enhanced the relative I^- selectivity (I/Cl = 2.1), consistent with pendrin mediating a larger component of the HCO_3^--dependent reacidification. Under physiological situations, luminal Cl^- levels probably remain much higher (30–50 mM). Thus, it is unlikely that CFTR contributes significantly to HCO_3^- flux across the apical membrane, a prediction supported by our fluid pH measurements (Fig. 7). The hypothesis that Calu-3 cells secrete HCO_3^- solely via CFTR clearly opposes our present findings. Our data do support a critical role for CFTR in "switching" Calu-3 cell HCO_3^- transport capability from pH_i regulatory (via basolateral AE) to HCO_3^- secretory modes (via activation of an apical AE) in response to cAMP elevation and activation of PKA (for discussion, see the legend to Fig. 8). This dual role of CFTR is particularly evident in the CFTR KD Calu-3 cells, where the reduced CFTR expression in these cells not only lowered the rate of cAMP-stimulated apical AE activity but also led to partial relief of basolateral AE inhibition normally seen in stimulated cells. Taken together, these observations suggest that CFTR participates in both processes. Furthermore, FRT cells expressing pendrin alone (Fig. 6) show a basal level of AE activity, which could not be further enhanced by cAMP elevation (Fig. 6, *D* and *E*). These results may indicate that in Calu-3 cells, CFTR tonically inhibits pendrin activity until a cAMP stimulus is received. Exactly how this occurs requires further clarification. Previous studies on CFTR and SLC26A3 and A6 transporters postulate physical interaction between the phosphorylated regulatory domain of CFTR with the STAS domain of the SLC26 transporters, which promote enhanced channel and AE activity (24). Co-expression studies in HEK cells showed that CFTR expression led to a marked increase in Cl^-/OH^- and Cl^-/HCO_3^- exchange mediated by SLC26A3, -A4, and -A6 (48). It is also possible that, under resting conditions, association between CFTR and pendrin blocks AE activity, a phenomenon recently described for Slc26a9 and the regulatory domain of CFTR in *Xenopus* oocyte co-expression studies (49).

The inhibition of the basolateral Cl^-/HCO_3^- exchanger under cAMP-elevated conditions fits with a primary role of this AE in maintaining pH_i. It is likely that the basolateral AE is also important for Cl^- accumulation under resting conditions, as has already been suggested for Calu-3 cells (33) as well as for HCO_3^--secreting pancreatic duct cells (50). Our results also suggest that GlyH-101 inhibition of CFTR in stimulated cells leads to the reactivation of the basolateral AE, possibly via the resulting alkalinization. This may help prevent an intracellular alkali load by shunting HCO_3^- accumulation by the basolateral Na^+-HCO_3^- cotransporter (NBC) (Fig. 8). The exact mechanisms involved in the cAMP/CFTR-dependent inhibition of the basolateral AE presently are not clear. AE2 is known to be very pH-sensitive (51). Thus, intracellular acidification produced by the efflux of HCO_3^- across the apical membrane upon fsk stimulation could provide the basis of one potential mechanism.

We obtained an insight into the role of the apical Cl^-/HCO_3^- exchanger in Calu-3 cells by examining the composition of the secreted fluid (Fig. 7). Our pH_i measurements predict fsk-stimulated, apical HCO_3^- secretion facilitated by pendrin-mediated Cl^-/HCO_3^- exchange. Forskolin-stimulated pendrin KD Calu-3 cells showed reduced apical AE activity and produced a fluid of lower pH, consistent with these predictions. Although CFTR knockdown or inhibition by GlyH-101 had no effect on the pH of fsk-stimulated secreted fluid, both maneuvers reduced the volume of secreted fluid. These findings are consistent with electrogenic Cl^- efflux via CFTR-driven transcellular fluid secretion and oppose the notion of HCO_3^- efflux through CFTR-driven fluid secretion, which is consistent with recent work on native serous cells isolated from pig and human SMGs (52). Cl^- secretion through CFTR is predicted to support apical Cl^-/HCO_3^- exchange by maintaining an inward Cl^- gradient for efficient anion exchange, which has also been observed for Slc26a3 (Dra) activity in mouse duodenum (53).

Our transcellular liquid secretion measurements showed that J_v was dependent on the presence of both Cl^- and HCO_3^- and was increased, dose-dependently, up to ~5-fold by fsk, in a time-dependent fashion (supplemental Fig. S6, *A* and *B*). We also found that much of the fluid secretion could be inhibited by basolateral anion transport inhibitors, H_2-DIDS and bumetanide (supplemental Fig. S6*C*), suggesting that Na^+, K^+, and Cl^- uptake via the basolateral Na^+-K^+-$2Cl^-$ cotransporter and HCO_3^- uptake via the basolateral NBC (and/or Cl^-/HCO_3^- exchange by basolateral AE2) support overall luminal fluid secretion from Calu-3 cells under cAMP-stimulated conditions

(Fig. 8). These results are in good agreement with previous studies on Calu-3 cells using a similar methodology (54) or the virtual gland model (55) and also with studies of intact SMGs (56, 57). In addition, we measured a maximal [HCO_3^-] in the fsk-stimulated secreted fluid of ~75 mM (pH 7.9), again very similar to the values obtained by Irokawa *et al.* (55) (80 mM). Computer modeling studies, based on data obtained in native pancreatic duct cells, indicate that a luminal concentration of HCO_3^- of this magnitude is compatible with an electroneutral Cl^-/HCO_3^- AE working in parallel with an electrogenic Cl^- channel, such as CFTR (58). The results of the present study are consistent with this model. Also, the results of our fluid secretion studies agree with previous investigations using intact SMG preparations from a range of species, which concluded that the active secretion of both HCO_3^- and Cl^- drives fluid secretion (16, 57). *In vitro* measurements in excised porcine bronchi suggested that airway fluid originates primarily from the SMG (59). More recently, *in vitro* optical studies from individual SMGs from pig and ferrets showed that cAMP agonists induced SMG fluid/mucus secretion by a combination of Cl^- and HCO_3^- secretion (56, 60). This process was reduced in transgenic CF ferrets and pigs (15, 61). Most studies of fluid secretion from human airway serous cells or SMGs suggest that secretion is dependent on apical Cl^- and HCO_3^- secretion through CFTR (14, 19, 46). This is consistent with the known expression of CFTR in SMG serous cells (52, 62). This also aligns with previous studies showing that the CFTR blocker, $CFTR_{inh}$-172 (63), inhibited pilocarpine- and forskolin-induced airway SMG secretion in pigs and humans without CF but not in human bronchi with CF (47). Interestingly, $CFTR_{Inh}$-172 had no effect on the pH of porcine SMGs gland fluid secretions under non-stimulated conditions (pH ~6.9) but lowered the pH of fluid secreted upon pilocarpine stimulation from ~7.1 to ~6.7, consistent with the inhibition of CFTR-dependent HCO_3^- secretion (47). However, these results could also be explained by CFTR working in parallel with an AE.

Physiologically, CFTR-regulated Cl^-/HCO_3^- exchange in airway SMGs may be important in maintaining the pH of the airway surface liquid. This is necessary for antimicrobial molecules and ultimately mucociliary clearance. Its absence could explain the acidic pH reported in CF airways, which would cause further detriment of lung defense (1, 2). Low pH could reduce ciliary beat frequency (9, 64), compromise bacterial clearance, and reduce antimicrobial activity of immune cells (10, 11). In CF, low pH could also "tighten" adhesive interactions between reported membrane-bound mucins and mucins of the mucus layer of the airway surface liquid (65). By altering the exposure of hydrophobic regions of the mucin molecules (66), the effectiveness of the mucus against harmful inhaled particles would be reduced. HCO_3^- secretion often accompanies mucus release, suggesting that HCO_3^- is required for proper mucus production (4–6). In addition, recent work indicates that HCO_3^- ions play an essential role in determining the final rheological properties of mucus via competing with fixed anions in mucins for Ca^{2+}. This ultimately regulates mucin swelling, cross-linking, and gel formation. Lack of HCO_3^- leads to the formation of thick, sticky, mucus, which strongly adheres to the lining epithelium (7, 8). In the context of the SMG and CF, lack of HCO_3^- would therefore predispose the glands to mucus blockage and damage, a characteristic sign of CF airway disease and an important mediator of lung pathophysiology. The recent finding that pendrin expression is coupled to mucin gene expression in response to inflammatory cytokines is important in that it suggests that mucus production and mucus expansion may be tightly co-regulated (42).

Mutations in the gene encoding pendrin lead to Pendred syndrome, a condition characterized by deafness and in some cases goiter, reflecting its expression in the inner ear and thyroid (67, 68). To our knowledge, Pendred syndrome patients have not been reported to develop disturbances in lung physiology. This may be because the lungs use other transporters to regulate HCO_3^- secretion, such as CFTR, in the absence of pendrin or because compensatory up-regulation of other SLC26A Cl^-/HCO_3^- exchangers occurs when pendrin is not present. A similar conclusion was reached in studies on pendrin in the kidney, where it functions in acid-base status (69, 70), yet no obvious renal abnormalities are observed in either Pendred patients or in *Slc26a4* knock-out mice (69, 70), Interestingly, the inflammatory cytokine, IL-4, up-regulates the functional expression of pendrin in primary cultures of human bronchial epithelial cells, whereby it mediates secretion of SCN^- and promotes the production of $OSCN^-$, a potent antimicrobial agent (30). Thus, in the context of airway serous SMGs, pendrin may also participate in Cl^--coupled SCN^- secretion in addition to HCO_3^- secretion.

In conclusion, our results are consistent with pendrin mediating the majority of HCO_3^- secretion across the apical membrane of Calu-3 monolayers via coupled exchange of Cl^- for HCO_3^-. This work establishes a critical and novel role for this anion exchanger in transporting HCO_3^- across human airway serous epithelial cells.

Acknowledgments—We thank Helen Glenwright for expert technical assistance. We also thank Luis Galietta and Olga Zegarra-Moran (University of Genoa, Italy) for supplying the FRT cells stably transfected with pendrin or CFTR.

REFERENCES

1. Coakley, R. D., Grubb, B. R., Paradiso, A. M., Gatzy, J. T., Johnson, L. G., Kreda, S. M., O'Neal, W. K., and Boucher, R. C. (2003) *Proc. Natl. Acad. Sci. U.S.A.* **100,** 16083–16088
2. Song, Y., Salinas, D., Nielson, D. W., and Verkman, A. S. (2006) *Am. J. Physiol. Cell. Physiol.* **290,** C741–C749
3. Quinton, P. M. (2008) *Lancet* **372,** 415–417
4. Garcia, M. A., Yang, N., and Quinton, P. M. (2009) *J. Clin. Invest.* **119,** 2613–2622
5. Holma, B., and Hegg, P. O. (1989) *Sci. Total Environ.* **84,** 71–82
6. Quinton, P. M. (2001) *Nat. Med.* **7,** 292–293
7. Chen, E. Y., Yang, N., Quinton, P. M., and Chin, W. C. (2010) *Am. J. Physiol. Lung Cell Mol. Physiol.* **299,** L542–L549
8. Muchekehu, R. W., and Quinton, P. M. (2010) *J. Physiol.* **588,** 2329–2342
9. Clary-Meinesz, C., Mouroux, J., Cosson, J., Huitorel, P., and Blaive, B. (1998) *Eur. Respir. J.* **11,** 330–333
10. Allen, D. B., Maguire, J. J., Mahdavian, M., Wicke, C., Marcocci, L., Scheuenstuhl, H., Chang, M., Le, A. X., Hopf, H. W., and Hunt, T. K. (1997) *Arch. Surg.* **132,** 991–996
11. Simchowitz, L. (1985) *J. Clin. Invest.* **76,** 1079–1089
12. Ostedgaard, L. S., Meyerholz, D. K., Chen, J. H., Pezzulo, A. A., Karp, P. H.,

Rokhlina, T., Ernst, S. E., Hanfland, R. A., Reznikov, L. R., Ludwig, P. S., Rogan, M. P., Davis, G. J., Dohrn, C. L., Wohlford-Lenane, C., Taft, P. J., Rector, M. V., Hornick, E., Nassar, B. S., Samuel, M., Zhang, Y., Richter, S. S., Uc, A., Shilyansky, J., Prather, R. S., McCray, P. B., Jr., Zabner, J., Welsh, M. J., and Stoltz, D. A. (2011) *Sci. Transl. Med.* **3,** 74ra24
13. Smith, J. J., and Welsh, M. J. (1992) *J. Clin. Invest.* **89,** 1148–1153
14. Choi, J. Y., Khansaheb, M., Joo, N. S., Krouse, M. E., Robbins, R. C., Weill, D., and Wine, J. J. (2009) *J. Clin. Invest.* **119,** 1189–1200
15. Khansaheb, M., Choi, J. Y., Joo, N. S., Yang, Y. M., Krouse, M., and Wine, J. J. (2011) *Am. J. Physiol. Lung Cell Mol. Physiol.* **300,** L370–L379
16. Wine, J. J., and Joo, N. S. (2004) *Proc. Am. Thorac. Soc.* **1,** 47–53
17. Devor, D. C., Singh, A. K., Lambert, L. C., DeLuca, A., Frizzell, R. A., and Bridges, R. J. (1999) *J. Gen. Physiol.* **113,** 743–760
18. Illek, B., Yankaskas, J. R., and Machen, T. E. (1997) *Am. J. Physiol.* **272,** L752–L761
19. Krouse, M. E., Talbott, J. F., Lee, M. M., Joo, N. S., and Wine, J. J. (2004) *Am. J. Physiol. Lung Cell Mol. Physiol.* **287,** L1274–L1283
20. Stewart, A. K., Yamamoto, A., Nakakuki, M., Kondo, T., Alper, S. L., and Ishiguro, H. (2009) *Am. J. Physiol. Gastrointest. Liver Physiol.* **296,** G1307–G1317
21. Melvin, J. E., Yule, D., Shuttleworth, T., and Begenisich, T. (2005) *Annu. Rev. Physiol.* **67,** 445–469
22. Singh, A. K., Riederer, B., Chen, M., Xiao, F., Krabbenhöft, A., Engelhardt, R., Nylander, O., Soleimani, M., and Seidler, U. (2010) *Am. J. Physiol. Cell Physiol.* **298,** C1057–C1065
23. Chen, W. Y., Xu, W. M., Chen, Z. H., Ni, Y., Yuan, Y. Y., Zhou, S. C., Zhou, W. W., Tsang, L. L., Chung, Y. W., Höglund, P., Chan, H. C., and Shi, Q. X. (2009) *Biol. Reprod.* **80,** 115–123
24. Ko, S. B., Zeng, W., Dorwart, M. R., Luo, X., Kim, K. H., Millen, L., Goto, H., Naruse, S., Soyombo, A., Thomas, P. J., and Muallem, S. (2004) *Nat. Cell Biol.* **6,** 343–350
25. Wheat, V. J., Shumaker, H., Burnham, C., Shull, G. E., Yankaskas, J. R., and Soleimani, M. (2000) *Am. J. Physiol. Cell Physiol.* **279,** C62–C71
26. Lohi, H., Kujala, M., Makela, S., Lehtonen, E., Kestila, M., Saarialho-Kere, U., Markovich, D., and Kere, J. (2002) *J. Biol. Chem.* **277,** 14246–14254
27. Bertrand, C. A., Zhang, R., Pilewski, J. M., and Frizzell, R. A. (2009) *J. Gen. Physiol.* **133,** 421–438
28. Shen, B. Q., Finkbeiner, W. E., Wine, J. J., Mrsny, R. J., and Widdicombe, J. H. (1994) *Am. J. Physiol.* **266,** L493–L501
29. MacVinish, L. J., Cope, G., Ropenga, A., and Cuthbert, A. W. (2007) *Br. J. Pharmacol.* **150,** 1055–1065
30. Pedemonte, N., Caci, E., Sondo, E., Caputo, A., Rhoden, K., Pfeffer, U., Di Candia, M., Bandettini, R., Ravazzolo, R., Zegarra-Moran, O., and Galietta, L. J. V. (2007) *J. Immunol.* **178,** 5144–5153
31. Rakonczay, Z., Jr., Hegyi, P., Hasegawa, M., Inoue, M., You, J., Iida, A., Ignáth, I., Alton, E. W., Griesenbach, U., Ovári, G., Vág, J., Da Paula, A. C., Crawford, R. M., Varga, G., Amaral, M. D., Mehta, A., Lonovics, J., Argent, B. E., and Gray, M. A. (2008) *J. Cell. Physiol.* **214,** 442–455
32. Inglis, S. K., Finlay, L., Ramminger, S. J., Richard, K., Ward, M. R., Wilson, S. M., and Olver, R. E. (2002) *J. Physiol.* **538,** 527–539
33. Loffing, J., Moyer, B. D., Reynolds, D., Shmukler, B. E., Alper, S. L., and Stanton, B. A. (2000) *Am. J. Physiol. Cell Physiol.* **279,** C1016–C1023
34. Dérand, R., Montoni, A., Bulteau-Pignoux, L., Janet, T., Moreau, B., Muller, J. M., and Becq, F. (2004) *Br. J. Pharmacol.* **141,** 698–708
35. Cobb, B. R., Ruiz, F., King, C. M., Fortenberry, J., Greer, H., Kovacs, T., Sorscher, E. J., and Clancy, J. P. (2002) *Am. J. Physiol. Lung Cell Mol. Physiol.* **282,** L12–L25
36. Dorwart, M. R., Shcheynikov, N., Yang, D., and Muallem, S. (2008) *Physiology* **23,** 104–114
37. Dossena, S., Vezzoli, V., Cerutti, N., Bazzini, C., Tosco, M., Sironi, C., Rodighiero, S., Meyer, G., Fascio, U., Fürst, J., Ritter, M., Fugazzola, L., Persani, L., Zorowka, P., Storelli, C., Beck-Peccoz, P., Bottà, G., and Paulmichl, M. (2006) *Cell. Physiol. Biochem.* **17,** 245–256
38. Mount, D. B., and Romero, M. F. (2004) *Pflugers Arch.* **447,** 710–721
39. Scott, D. A., Wang, R., Kreman, T. M., Sheffield, V. C., and Karniski, L. P. (1999) *Nat. Genet.* **21,** 440–443
40. Shcheynikov, N., Yang, D., Wang, Y., Zeng, W., Karniski, L. P., So, I., Wall, S. M., and Muallem, S. (2008) *J. Physiol.* **586,** 3813–3824
41. Royaux, I. E., Suzuki, K., Mori, A., Katoh, R., Everett, L. A., Kohn, L. D., and Green, E. D. (2000) *Endocrinology* **141,** 839–845
42. Nakao, I., Kanaji, S., Ohta, S., Matsushita, H., Arima, K., Yuyama, N., Yamaya, M., Nakayama, K., Kubo, H., Watanabe, M., Sagara, H., Sugiyama, K., Tanaka, H., Toda, S., Hayashi, H., Inoue, H., Hoshino, T., Shiraki, A., Inoue, M., Suzuki, K., Aizawa, H., Okinami, S., Nagai, H., Hasegawa, M., Fukuda, T., Green, E. D., and Izuhara, K. (2008) *J. Immunol.* **180,** 6262–6269
43. Satoh, H., Susaki, M., Shukunami, C., Iyama, K., Negoro, T., and Hiraki, Y. (1998) *J. Biol. Chem.* **273,** 12307–12315
44. Shcheynikov, N., Wang, Y., Park, M., Ko, S. B., Dorwart, M., Naruse, S., Thomas, P. J., and Muallem, S. (2006) *J. Gen. Physiol.* **127,** 511–524
45. Scott, D. A., and Karniski, L. P. (2000) *Am. J. Physiol. Cell Physiol.* **278,** C207–C211
46. Lee, M. C., Penland, C. M., Widdicombe, J. H., and Wine, J. J. (1998) *Am. J. Physiol.* **274,** L450–L453
47. Thiagarajah, J. R., Song, Y., Haggie, P. M., and Verkman, A. S. (2004) *FASEB J.* **18,** 875–877
48. Ko, S. B., Shcheynikov, N., Choi, J. Y., Luo, X., Ishibashi, K., Thomas, P. J., Kim, J. Y., Kim, K. H., Lee, M. G., Naruse, S., and Muallem, S. (2002) *EMBO J.* **21,** 5662–5672
49. Chang, M. H., Plata, C., Sindic, A., Ranatunga, W. K., Chen, A. P., Zandi-Nejad, K., Chan, K. W., Thompson, J., Mount, D. B., and Romero, M. F. (2009) *J. Biol. Chem.* **284,** 28306–28318
50. Ishiguro, H., Naruse, S., Kitagawa, M., Mabuchi, T., Kondo, T., Hayakawa, T., Case, R. M., and Steward, M. C. (2002) *J. Physiol.* **539,** 175–189
51. Stewart, A. K., Kurschat, C. E., Burns, D., Banger, N., Vaughan-Jones, R. D., and Alper, S. L. (2007) *Am. J. Physiol. Cell Physiol.* **292,** C909–C918
52. Lee, R. J., and Foskett, J. K. (2010) *J. Clin. Invest.* **120,** 3137–3148
53. Simpson, J. E., Gawenis, L. R., Walker, N. M., Boyle, K. T., and Clarke, L. L. (2005) *Am. J. Physiol. Gastrointest. Liver Physiol.* **288,** G1241–G1251
54. Ramesh Babu, P. B., Chidekel, A., Utidjian, L., and Shaffer, T. H. (2004) *Biochem. Biophys. Res. Commun.* **319,** 1132–1137
55. Irokawa, T., Krouse, M. E., Joo, N. S., Wu, J. V., and Wine, J. J. (2004) *Am. J. Physiol. Lung Cell Mol. Physiol.* **287,** L784–L793
56. Joo, N. S., Saenz, Y., Krouse, M. E., and Wine, J. J. (2002) *J. Biol. Chem.* **277,** 28167–28175
57. Ballard, S. T., and Inglis, S. K. (2004) *J. Physiol.* **556,** 1–10
58. Sohma, Y., Gray, M. A., Imai, Y., and Argent, B. E. (2000) *J. Membr. Biol.* **176,** 77–100
59. Ballard, S. T., Trout, L., Bebök, Z., Sorscher, E. J., and Crews, A. (1999) *Am. J. Physiol.* **277,** L694–L699
60. Cho, H. J., Joo, N. S., and Wine, J. J. (2010) *Am. J. Physiol. Lung Cell Mol. Physiol.* **299,** L124–L136
61. Joo, N. S., Cho, H. J., Khansaheb, M., and Wine, J. J. (2010) *J. Clin. Invest.* **120,** 3161–3166
62. Engelhardt, J. F., Yankaskas, J. R., Ernst, S. A., Yang, Y., Marino, C. R., Boucher, R. C., Cohn, J. A., and Wilson, J. M. (1992) *Nat. Genet.* **2,** 240–248
63. Ma, T., Thiagarajah, J. R., Yang, H., Sonawane, N. D., Folli, C., Galietta, L. J., and Verkman, A. S. (2002) *J. Clin. Invest.* **110,** 1651–1658
64. Schmid, A., Sutto, Z., Schmid, N., Novak, L., Ivonnet, P., Horvath, G., Conner, G., Fregien, N., and Salathe, M. (2010) *J. Biol. Chem.* **285,** 29998–30007
65. Matsui, H., Grubb, B. R., Tarran, R., Randell, S. H., Gatzy, J. T., Davis, C. W., and Boucher, R. C. (1998) *Cell* **95,** 1005–1015
66. Bhaskar, K. R., Gong, D. H., Bansil, R., Pajevic, S., Hamilton, J. A., Turner, B. S., and LaMont, J. T. (1991) *Am. J. Physiol.* **261,** G827–G832
67. Everett, L. A., Glaser, B., Beck, J. C., Idol, J. R., Buchs, A., Heyman, M., Adawi, F., Hazani, E., Nassir, E., Baxevanis, A. D., Sheffield, V. C., and Green, E. D. (1997) *Nat. Genet.* **17,** 411–422
68. Everett, L. A., Morsli, H., Wu, D. K., and Green, E. D. (1999) *Proc. Natl. Acad. Sci. U.S.A.* **96,** 9727–9732
69. Royaux, I. E., Wall, S. M., Karniski, L. P., Everett, L. A., Suzuki, K., Knepper, M. A., and Green, E. D. (2001) *Proc. Natl. Acad. Sci. U.S.A.* **98,** 4221–4226
70. Wall, S. M., and Pech, V. (2008) *Curr. Opin. Nephrol. Hypertens.* **17,** 18–24